14th International Symposium on Turbulence and Shear Flow Phenomena (TSFP14)
Heidelberg, Germany, July 28–31, 2026

WAKE STRAIGHTENING BEHIND TWO STAGGERED PITCHING FOILS

Priscila Portocarrero[1,a] **Muhammad Saif Ullah Khalid** [2,b] **Arman Hemmati**[3,a]
[a] Department of Mechanical Engineering, University of Alberta, Edmonton, AB, T6G 2R3, Canada
[b] Department of Mechanical and Mechatronics Engineering, Lakehead University, Thunder Bay, ON, P7B 5E1, Canada
pportoca@ualberta.ca [1], mkhalid7@lakeheadu.ca [2], arman.hemmati@ualberta.ca[3]

SYNOPSIS

The mechanism of wake deflection behind two staggered pitching foils is numerically investigated within a range of Reynolds numbers ($1000 < Re < 10000$), horizontal ($1c < h < 3c$) and vertical ($0.75c < v < 1c$, where c is the foil chord) separation distances, and phase differences ($0° < \phi < 180°$) at Strouhal number (St) of 0.3 and 0.4. Two-dimensional incompressible Navier Stokes and Continuity equations were solved directly using OpenFOAM. Two flow patterns are identified: merged and separated wakes. In the separated wake pattern, we observe two distinct behaviors described as straightened and deflected wakes. The first one presents evenly distributed vortices along the wake before interacting with the wake behind the neighbor foil. The latter presents rearranged vortex pairs that bends the wake towards the neighbor foil. This study aims to characterize the wake given by a range of phase differences in staggered pitching foils and relate it to its propulsive performance.

INTRODUCTION

Fish schools are biological systems that, beyond offering reproductive and predation advantages (Weihs, 1973), also provide hydrodynamic benefits by improving efficiency and reducing power consumption in collective swimming. These benefits have attracted the attention of engineers, who aim to apply schooling patterns and kinematics to various technologies, such as wind turbines, Micro Aerial Vehicles, and Autonomous Underwater Vehicles (Guo *et al.*, 2023). In order to improve existing flow control strategies and develop new technologies, we should fully explore the vortex dynamics behind these arrangements. Several investigations have defined vortex structures and wake patterns behind a single oscillating body, such as the well-known Benard–von Karman street (BvK). This wake presents different two-dimensional transitions from BvK to reverse BvK, and from reverse BvK to deflected reverse BvK. Wake deflections present a rearrangement of vortex pairs along a vortex street that allows downward or upward bending (Deng *et al.*, 2016, Zurman-Nasution *et al.*, 2020).

Interactions between deflected wakes formed behind parallel (side-by-side) and staggered foil schools have been studied over the years. Dewey *et al.* (2014) experimentally studied two side-by-side oscillating foils at Re = 4700, St = 0.25, $\phi =$ 0°-360°, and separation distances from $0.5c$ to $2c$. They explored the formation mechanism of both separated and merged wakes. However, their study did not provide quantitative models or evidence for these mechanisms. More recently, Gungor *et al.* (2022) conducted two-dimensional simulations of side-by-side oscillating foils at $Re = 4000$, exploring various horizontal and vertical separation distances and phase angles from 0° to 180°. They observed both merged and separated wakes, and identified kinematic and geometric thresholds associated with their formation and evolution. Moreover, they developed a mathematical model to predict wake merging based on wake deflection. However, their model did not consider staggered configurations with horizontal offsets. The current study aims to model the wake formation behind staggered pitching foils across a range of phase differences. Huera-Huarte (2018) experimentally investigated staggered pitching foils, both in-phase and out-of-phase, at Re up to 24000, and identified two wake patterns behind the system: merged and separated. Although this study evaluated performance and wakes for two staggered foils, it did not explore a range of phase differences or explain wake interactions. More recently, Portocarrero *et al.* (2025) identified and characterized wake patterns behind staggered in-phase pitching foils at $Re = 1000 - 10000$. They explained the mechanism of formation of wake patterns based on the balance of induced velocities and rearrangement of vortex pairs in the wake. However, that study focused only on in-phase pitching motion, while the current study aims to model wake formation behind staggered foils in a wider parameter space, including phase differences

This study explores the deflection of evolving wakes behind two staggered pitching foils. We observed that both foil proximity and synchronization (phase difference) are important in dictating interactions between wakes, including what we refer to as wake-straightening. This feature was not observed in side-by-side or single pitching foils. These findings offer new insights into wake dynamics in staggered foil school configurations, which can contribute to improving the performance of bio-inspired systems.

COMPUTATIONAL METHODOLOGY

Simulations were carried out in OpenFOAM using Overset Grid Assembly (OGA) technique to directly solve two-dimensional incompressible Continuity and Navier-Stokes equations at $Re = 1000 - 10000$. The computational domain extended by $30c$ in the streamwise (x) and $16c$ in the cross-flow (y) direction. Leading edge of the leading foil was located at 8c from the inlet, where c is the foil chord length. Vertical ($v^* = v/c$) and horizontal ($h^* = h/c$) positions of the follower foil ranged from 0.75c to 1c, and 1c to 3c from the leader foil trailing edge, respectively. A non-homogeneous grid with 7×10^5 hexahedral elements was constructed for these simulations. The inlet was assigned the Dirichlet boundary condition and the outlet boundary condition was Neumman outflow condition. Top and bottom boundaries were set as slip walls, and the foil surface was prescribed with no-slip wall condition.

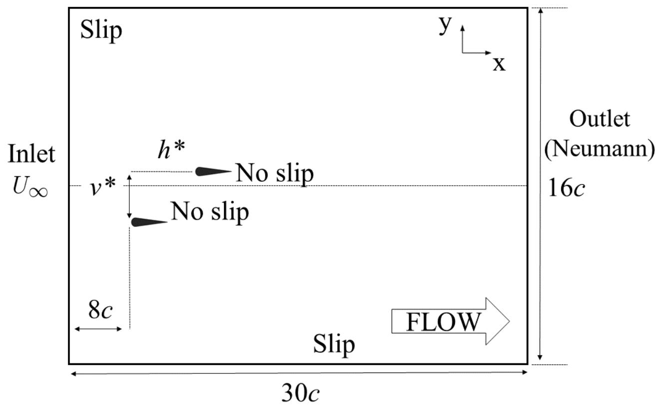

Figure 1: 2-D computational domain of two-fish school in staggered configuration with boundary conditions (not to scale).

The Courant number remained below 0.8 for all the simulations, and the convergence threshold was set to 10^{-5}. The verification and validation studies are reported in Verma *et al.* (2022). Two teardrop foils in staggered configuration, shown in Figure 1, oscillated following a sinusoidal motion profile represented by $\theta_1(t) = \theta_0 sin(2ft)$ and $\theta_2(t) = \theta_0 sin(2ft+\phi)$ where θ_0 is the pitching amplitude (fixed at 8°). Subscripts 1 and 2 represents pitching motion of Foil 1 and Foil 2, respectively. The Strouhal number ranged from 0.3 to 0.4. The phase difference (ϕ) ranges from 0° to 180° with increments of 30°. A summary of the kinematic and geometric parameters is found in Table 1.

Table 1: Parametric space of simulations

x/c	y/c	St	Re	θ_0
1-3	0.75-1	0.3-0.4	1000-10000	8°

RESULTS AND DISCUSSION

We analyze the wake interactions and vortex dynamics behind staggered foils for a range of phase differences using quantitative and qualitative approaches. Normalized contours of vorticity and circulation of flow structures are evaluated to categorize different wake topologies. Types of wake deflections are identified and classified in these topologies both qualitatively and quantitatively. Also, propulsive performance is studied to evaluate its correspondence with wake patterns.

Wake straightening identification

Two wake patterns are observed behind the system of two staggered foils: merged and separated wakes, as shown by the normalized spanwise vorticity contours in Figure 2. Merged wakes are characterized by two vortex streets that coalesce into a single jet at the center (Figure 2a). Contrarily, separated wakes show vortex streets that initially interact but diverge from each other (Figure 2b). This is consistent with the observations of Huera-Huarte (2018). These patterns are formed due to the interaction between vortices from both streets, which leads to the rearrangements of vortex pairs and

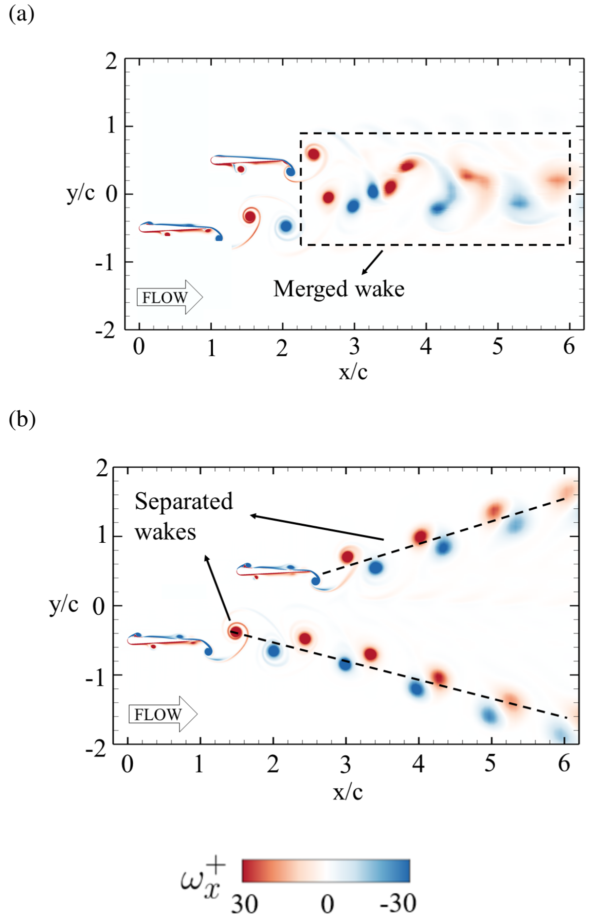

Figure 2: Contours of normalized spanwise vorticity (ω_z^+) of staggered foils for (a) h^*=1, v^*=1, $St = 0.4$, ϕ=0°, (b) h^*=1.5, v^*=1, $St = 0.4$, ϕ=0°, at $Re = 4000$

variations in their convective velocities. This mechanism is further explained in our previous study (Portocarrero *et al.*, 2025) for in-phase pitching foils.

Figure 3 depicts the classification of wake patterns behind two-staggered foil systems separated by 1c and 0.75c in a wake map at a range of h^* and ϕ at $St = 0.4$ and 0.3. As was previously observed by Portocarrero *et al.* (2024), there is a periodicity in the occurrence of wake patterns with respect to h^*. This alternating behavior is due to the interaction between co-rotating and counter-rotating vortices, which changes with the horizontal offset (proximity) between foils. Regarding phase differences, both wake maps are divided into two groups: 0° to 60° (Group A) and 90° to 180° (Group B). Wake patterns in the first group are the inverse of those in the second group. This reversal is caused by the change in the direction of pitching of the follower foil. Since phase angles in each group are supplementary, they produce opposite wake patterns. However, we observed differences in how vortex pairs are arranged over time when comparing separated wake patterns from both groups. To explain this rearrangement of structures, we identify straightening in the first group and deflections in the second group. This phenomenon highlights how vortex interactions differ in separated wake patterns depending on the phase difference.

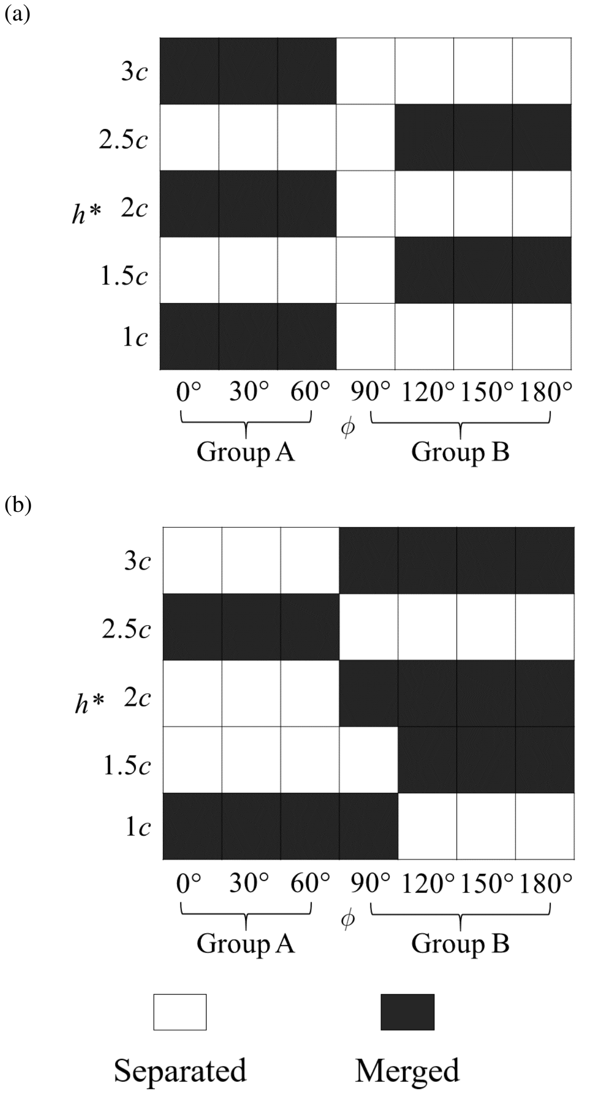

Figure 3: Classification of wake patterns of foils in staggered configuration for $Re = 4000$ and a range of vertical and horizontal separation distances at (a) $St = 0.4$ and (b) $St = 0.3$.

Based on the observable changes in wake pattern, we identify this phenomenon as Proximity-Induced Wake Deflection (PIWD), where the wake of the primary foil is deflected away or towards the neighboring foil. The PIWD phenomenon leads to Wake Straightening (WS) within a particular parameter space, where the wake becomes undeflected, or straight, within the horizontal gap with the neighboring foil. Following the interaction with the neighboring foil, however, the wake changes its convective direction, depending on the greater induced effects. We identify straight wakes in the first group and deflected wakes in the second group. This phenomenon highlights how vortex interactions differ in separated wake patterns depending on the phase difference. Further inspection reveals that the primary wake is in fact deflected towards the neighboring foil, leading to straightening of its vortex street. Up to interacting with the wakes of the neighboring foil, this effect is altered depending on the foils kinematics and wake dynamics.

To distinguish WS in wake patterns behind staggered foils, Figure 4 shows contours of normalized spanwise vorticity for three cases: (a) h^*=2, v^*=1, $St = 0.3$, ϕ=0°, (b) h^*=1, v^*=1, $St = 0.4$, ϕ=90°, and (c) $St = 0.4$. A straightened wake is shown in Figure 4a , and a deflected wake towards the neighbor foil is shown in Figures 4b. This is called pro-neighbor deflected (PnD) wake. On the left side, vortex pairs are evenly spaced within the vortex street, before interacting with the neighboring wake. After interaction, they rearrange and change the orientation of the wake away from

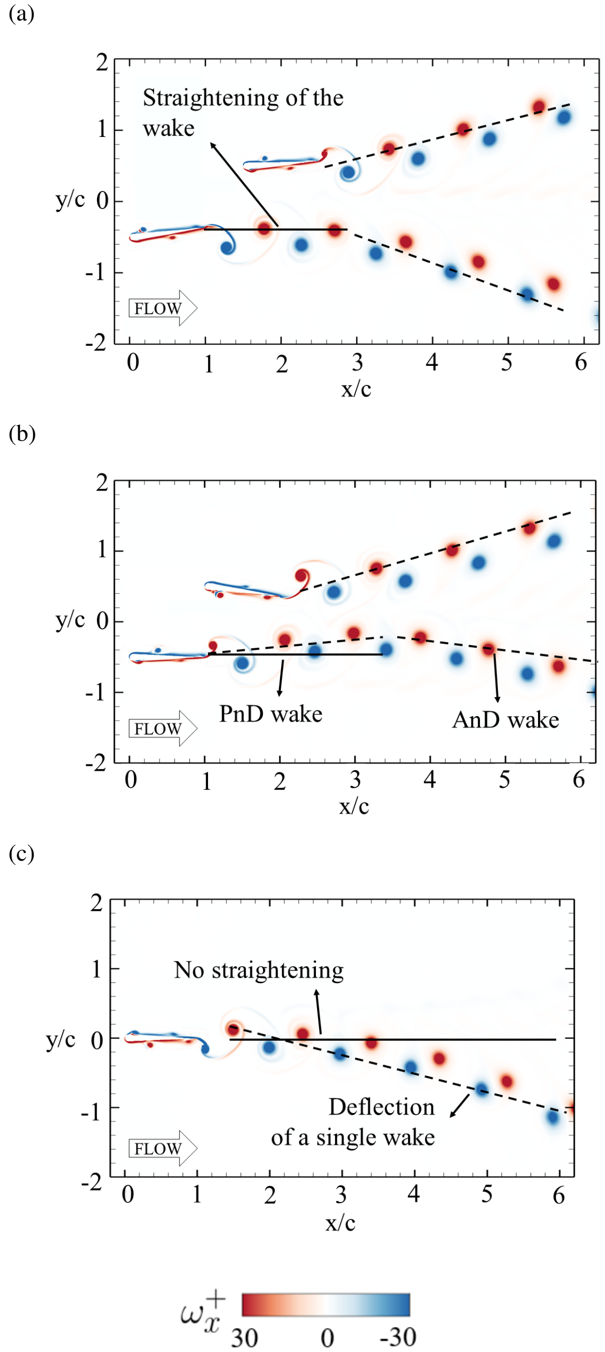

Figure 4: Contours of normalized spanwise vorticity (ω_z^+) of staggered foils for (a) straightened wake ($St = 0.4$, $v^* = 1$, $h^* = 1.5$, ϕ=60°), (b) pro-neighbor deflected wake ($St = 0.4$. $v^* = 1$, $h^* = 1$, ϕ=90°) and (c) deflected wake behind a single foil ($St = 0.4$), at $Re = 4000$.

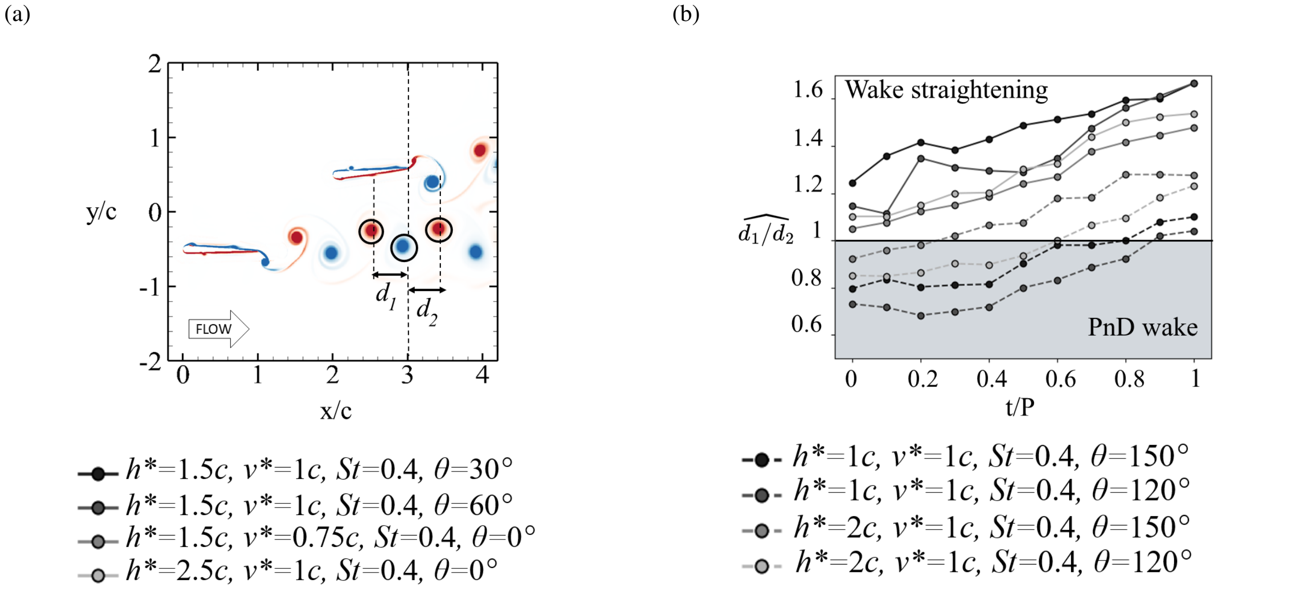

Figure 5: (a) Parameters used in the proposed criteria (b) Ratio of cycle-averaged distances $\widehat{d_1/d_2}$ of pairs of vortices of straightened and PnD wakes during a pitching cycle at $Re = 4000$. Legend of vorticity contours in Figure 4 is used here.

the neighbor. This is called anti-neighbor deflected (AnD) wake. On the right side, vortex pairs initially appear to deflect towards the neighbor foil, as if the wakes are about to merge. However, vortex pairs rearrange again after interacting with the neighbor wake, resulting in AnD wake. This is the first reported observation of wake straightening triggered by the interaction of two vortex streets due to foil proximity in school configuration. Figure 4c depicts wake of a single pitching foil at $St = 0.4$, where straightening is not triggered due to the absence of a neighboring wake.

The ratio of cycle-averaged distances d_1 and d_2 in the wake, as shown in Figure 5, was measured during one pitching cycle for both straightened and PnD wakes. Figure 5 shows that d_1 increases while d_2 decreases for straightened wakes, indicating a stable vortex arrangement over time ($d_1/d_2 > 1$). In contrast, PnD wakes exhibit a rearrangement of vortex pairs early in the cycle: d_1 decreases and d_2 increases ($d_1/d_2 < 1$). A clear threshold is observed at a ratio of one. When the ratio exceeds unity, it indicates that the angle of wake deflection has changed due to a shift in the resultant convective velocity. This reflects a change in vortex pairings over time. This analysis provides the first quantitative description of wake straightening caused by the interaction between two vortex streets.

We now explore the cases of lower and upper limits of Re. Figure 6 depicts contours of normalized spanwise vorticity of straightened and PnD wakes for Re = 1000 and Re = 10000. Straightened wakes, shown in Figures 6a and 6b, present evenly distributed vortices before interacting with the neighboring wake similar to Figure 4. PnD wakes shown in Figures 6c and 6d present arranged vortex pairs that bend the wake. These vortex pairs maintained their structure and dynamics, as shown in Figure 4 for Re = 4000. This demonstrates that wake straightening phenomenon and its formation mechanism remains consistent within the range of Re = 1000 - 10000.

Propulsive performance

We now study the relation between propulsive performance and straigthening behind in-phase pitching staggered foils by analyzing performance parameters. Figure 7 depicts cycle-averaged thrust ($\widetilde{C_T}$), power coefficients ($\widetilde{C_P}$) and efficiency (η) for the system (average of both foils) at $St = 0.3$ and 0.4, and a range of h^* and v^* at Re = 4000 showing straightened and PnD wake patterns. These parameters are analyzed over a large number of oscillations until the system reaches a quasi-steady state, which is highlighted in gray. We aim to evaluate how different wake patterns affect the system propulsive performance. To ensure statistical convergence, we discard the ten cycles to eliminate developmental stages, as recommended by Gungor *et al.* (2022). Figure 7a shows that thrust coefficient is similar for both straightened and PnD wakes at the same St. However, $\widetilde{C_P}$ shows differences in Figure 7b where coefficients are larger for PnD wakes. Consequently, efficiency is smaller for PnD wake cases and larger for straightened wake cases, as depicted in Figure 7c.

These differences can be associated to the kinematics and flow dynamics. In both wake regimes, the in-phase pitching motion produces comparable thrust values. This suggests that the net streamwise momentum remains similar across cases (He *et al.*, 2023). This observation is consistent with the momentum flux analysis, which does not show significant differences between straightened and PnD wakes. However, the higher power coefficients observed in PnD cases indicate that additional energetic costs are associated with these wake patterns (Modali *et al.*, 2021). This suggests the flow structures generated in PnD wakes involve more complex velocity fields, including stronger vortex interactions.

These findings provides design insights for applications such as bio-inspired propulsion systems and energy harvesting devices (Dewey *et al.*, 2014). For propulsive systems, such as underwater vehicles or robotic swimmers, straightened wake regimes are advantageous as they maximize efficiency by decreasing power consumption.

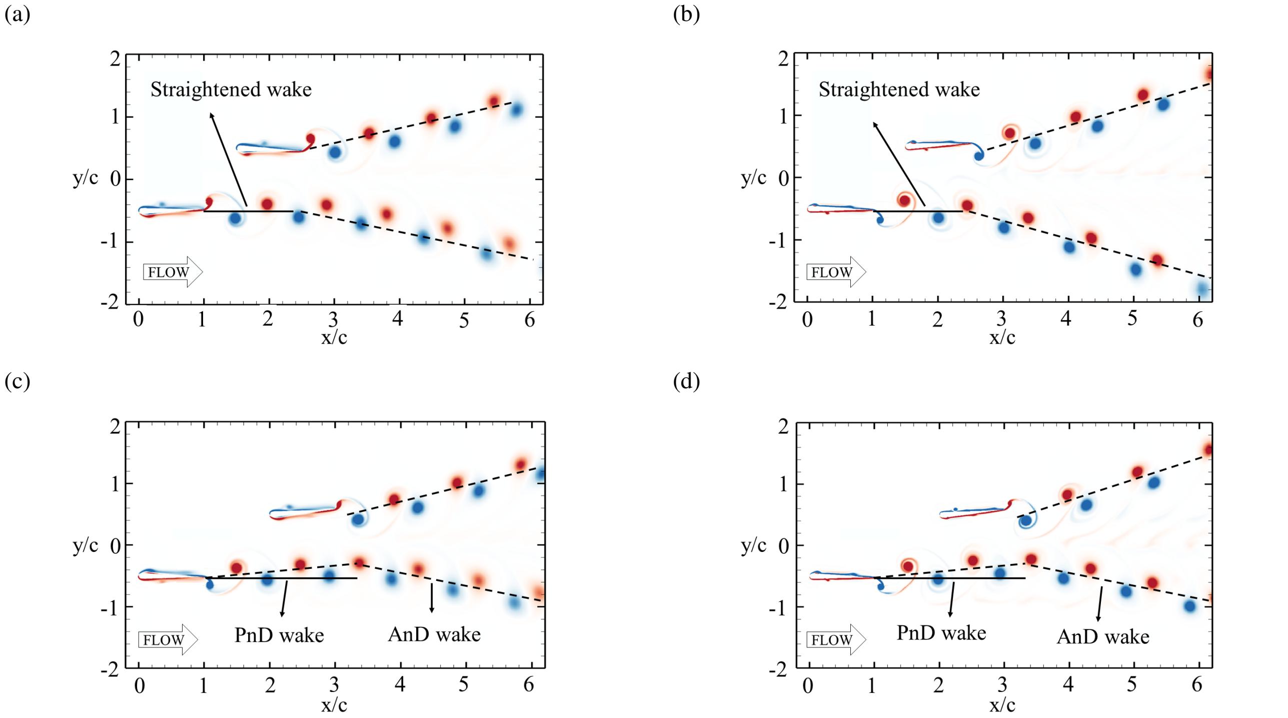

Figure 6: Contours of normalized spanwise vorticity of staggered foils for straightened wake ($St = 0.4$, $v^* = 1.5$, $h^* = 1$, $\phi = 30$) at (a) $Re = 1000$, (b) $Re = 10000$, and PnD wake ($St = 0.4$, $v^* = 2$, $h^* = 1$, $\phi = 120$) at (c) $Re = 1000$, (d) $Re = 10000$. Legend of vorticity contours in Figure 4 is used here.

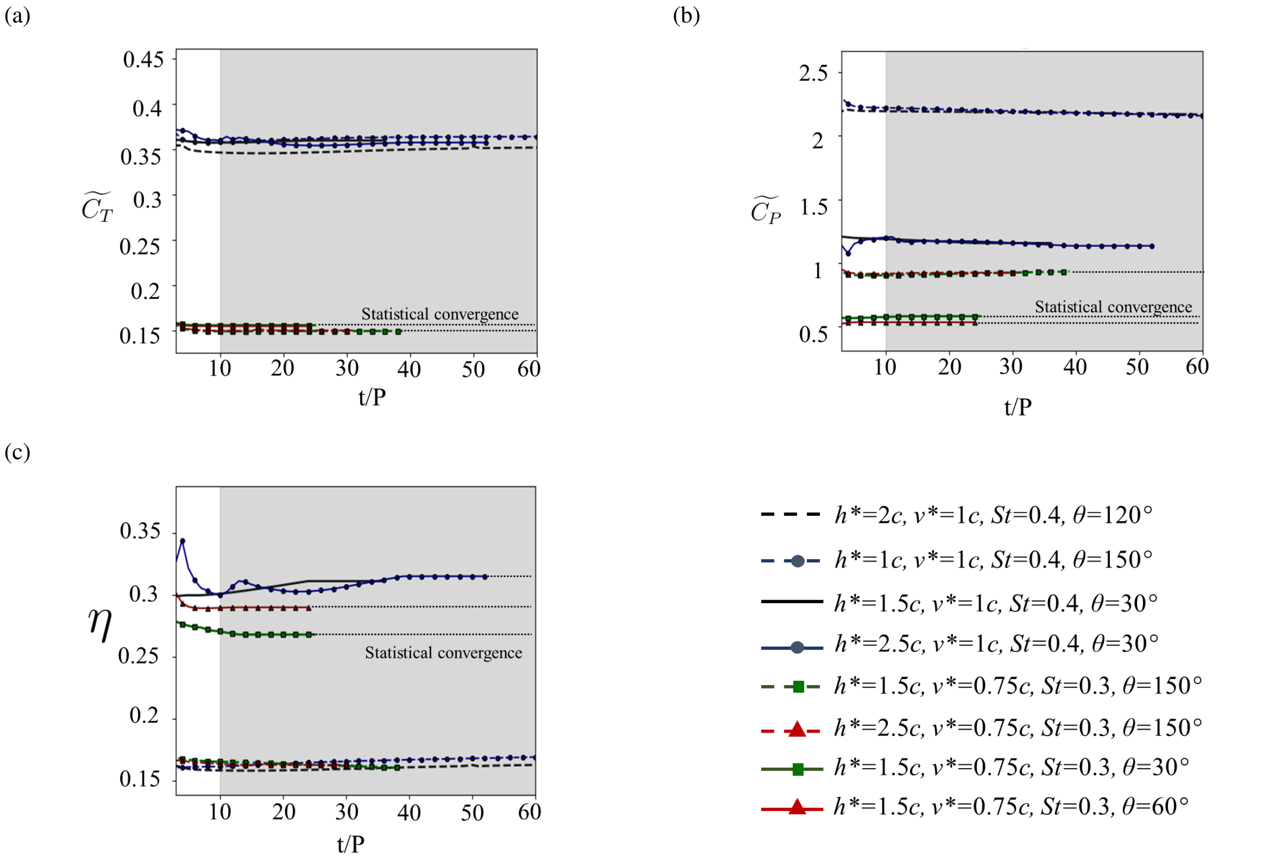

Figure 7: Cycle-averaged (a) thrust ($\widetilde{C_T}$), (b) power coefficients ($\widetilde{C_P}$) and (c) efficiency (η) of the system (averaged of both foils) at a range of St, h^*, v^* and ϕ, at $Re = 4000$. The dotted line added to the end of each case reflected projection of quasi-steady behavior.

CONCLUSIONS

Numerical simulations on the flow around two staggered pitching foils are evaluated at different Strouhal numbers (0.3 and 0.4), horizontal separation distances ($1 < h^* < 3$), vertical separation distances ($0.75 < v^* < 1$), phase differences ($0<\phi<180$) and *Re* (1000 - 10000). Separated wake exhibits a newly discovered wake straightening phenomenon. There are wake straightening and deflections observed in the wake, which belong to particular ranges of phase-differences. Their formation depends on the foil synchronization and wake positioning. Straightening is present in group A of phase differences which ranges from 0° to 60°. Pro-neighbor deflected wake (PnD) is present in group B of phase differences which ranges from 90° to 180°. Straightening presents evenly distributed vortices along the wake before interacting with the neighbor wake. PnD wake present rearranged vortex pairs that triggers an induced velocity that deflects the wake towards the neighbor foil, suggesting an initial tendency to merge. Finally, the propulsive performance analysis indicated that both wake patterns are associated with the same thrust production. However, straightened wakes demonstrate lower power consumption and larger efficiency compared to PnD wakes.

REFERENCES

Deng, Jian, Sun, Liping, Teng, Lubao, Pan, Dingyi & Shao, Xueming 2016 The correlation between wake transition and propulsive efficiency of a flapping foil: A numerical study. *Physics of Fluids* **28** (9), 094101.

Dewey, Peter A., Quinn, Daniel B., Boschitsch, Birgitt M. & Smits, Alexander J. 2014 Propulsive performance of unsteady tandem hydrofoils in a side-by-side configuration. *Physics of Fluids* **26** (4), 041903.

Gungor, Ahmet, Khalid, Muhammad Saif Ullah & Hemmati, Arman 2022 Classification of vortex patterns of oscillating foils in side-by-side configurations. *Journal of Fluid Mechanics* **951**, A37.

Guo, Jiacheng, Zhang, Wei, Han, Pan, Fish, Frank E & Dong, Haibo 2023 Thrust generation and propulsive efficiency in dolphin-like swimming propulsion. *Bioinspiration & Biomimetics* **18** (5), 056001.

He, Ruiyang, Deng, Xiaowei, Li, Yichun, Dong, Zhikun, Gao, Xiaoxia, Lu, Lin, Zhou, Yue, Wu, Jianzhong & Yang, Hongxing 2023 Three-dimensional yaw wake model development with validations from wind tunnel experiments. *Energy* **282**, 128402.

Huera-Huarte, F.J. 2018 Propulsive performance of a pair of pitching foils in staggered configurations. *Journal of Fluids and Structures* **81**, 1–13.

Modali, Pranav K., Vinod, Ashwin & Banerjee, Arindam 2021 Towards a better understanding of yawed turbine wake for efficient wake steering in tidal arrays. *Renewable Energy* **177**, 482–494.

Portocarrero, Priscila, Gungor, Ahmet & Hemmati, Arman 2025 Mechanism of formation of wake patterns behind two staggered in-phase pitching foils. *Bioinspiration Biomimetics* **20** (6), 066013.

Verma, Suyash, Khalid, Muhammad S.U. & Hemmati, Arman 2022 On association of lift generation, wake topology and kinematics of oscillating foils. *International Journal of Micro Air Vehicles* **14**, 17568293211073959.

Weihs, D. 1973 Hydromechanics of fish schooling. *Nature* **241** (5387), 290–291.

Zurman-Nasution, A. N., Ganapathisubramani, B. & Weymouth, G. D. 2020 Influence of three-dimensionality on propulsive flapping. *Journal of Fluid Mechanics* **886**, A25.